24th INTERNATIONAL CONGRESS ON SOUND AND VIBRATION
23–27 July 2017, London

ROBUST ESTIMATION OF THE ENERGY FLOW IN TIMBER STRUCTURES

Christoph Winter, Martin Buchschmid and Gerhard Müller
Chair of Structural Mechanics, Technical University of Munich, Arcisstr. 21, 80333 München, Germany
email: christoph.winter@tum.de

Within the context of efficient and sustainable design of buildings, a trend towards lightweight structures, e.g. timber structures, is recognizable. This trend implies the necessity of being able to predict serviceability and comfort as well as sound transmission in order to fulfill building requirements. To generate reliable prediction methods, the transfer of energy between building components has to be investigated. The Finite Element Method (FEM) is a convenient tool to predict the vibroacoustic behavior. However, without appropriate post-processing it is limited due to the sensitivity of the results at higher frequencies. In the mid-frequency range a sufficient number of modes per band enables the use of statistical methods like the Statistical Energy Analysis (SEA). It delivers averaged results and thus copes with the sensitivity. But the SEA is always limited to the governing partial differential equation related to wave types of the structures. E.g. through-thickness effects of plate-like structures at high frequencies are not modeled. As both techniques have a restricted validity regarding the frequency range, averaging techniques of the SEA are applied in the post-processing of the FEM to obtain an adapted hybrid approach. In case the load is unknown a robust estimation of the energy flow is needed for a general prognosis. The SEA delivers an ensemble average, but only within a limited frequency range, whereas one realization of the Energy Flow Analysis (EFA) simulates one specific load case. By averaging over varying random load cases, the EFA is able to predict the energy flow - which is robust regarding the load - inside a certain confidence interval. This contribution will focus on the statistical behavior of the energy flow due to variation of the number of loads and realizations. Furthermore, a comparison with a SEA model will be performed.

Keywords: Energy Flow Analysis, Statistical behavior, Timber structures, Finite Element Method.

1. Introduction

A trend towards lightweight structures within the context of efficient and sustainable design of buildings, e.g. timber structures, is recognizable. This trend implies the necessity of being able to predict serviceability and comfort as well as sound transmission in order to fulfill vibroacoustic requirements. To generate reliable prediction methods, the transfer of energy between building components has to be investigated.

In the low frequency range, the Finite Element Method (FEM) is suitable for structural dynamic predictions. As the frequency rises, the number of modes per frequency band increases, whereby the classical FEM is limited by the sensitivity of the results and the application of statistical methods becomes necessary. The Statistical Energy Analysis (SEA) provides robust results for the mid-frequency range for a sufficient number of modes per band, but generally allows only restricted resolution in space and frequency. Furthermore, the SEA is typically not able to represent through-thickness effects of plate-like structures at high frequencies. Hence, for the prediction averaging methods of SEA

[1] are applied within the framework of an Energy Flow Analysis (EFA) in the subsequent evaluation of the FEM for the aforementioned structures [2, 3].

In case the load is unknown a robust estimation of the energy flow is needed for a general prognosis. The SEA delivers an ensemble average, but only within a limited frequency range, whereas one realization of the EFA simulates one specific load case. By averaging over varying random load cases, the EFA is able to predict the energy flow - which is robust regarding the load - inside a certain confidence interval. This contribution will focus on the statistical behavior of the energy flow due to variation of the number of loads and realizations. Furthermore, a comparison with a SEA model will be performed. The investigations are part of the joint research project "Vibroacoustics in the planning process for timber constructions" (18726N) funded by the German Research Foundation (DFG) and German Federation of Industrial Research Associations (AiF).

2. Energy Flow Analysis

For the application of the EFA, the structure is divided into subsystems in accordance with their subdivision into components whereby, in contrast to the SEA, the prerequisite of the so-called weak coupling is not imperative and the subsystem definition is independent on wave types.

First of all, a harmonic analysis is performed, whereby the subsystems are excited separately. Therefore, pressure is applied on selected elements, instead of using nodal loads, to be able to build up planar excitations like air-borne sound pressure more realistically and especially to avoid that singularities affect the resulting input power. The latter is calculated by integrating over the product of the applied pressure p and the resulting velocity $v_{e,k}$ at the nodes k connected to the loaded elements e. Therefore, both values as well as the coordinates x and y are approximated across the element's area by the $n_N = 8$ quadratic ansatz functions $N_{e,i}$. In case of the velocity this leads to:

$$v_e = \sum_{i=1}^{n_N} v_{e,i} \cdot N_{e,i} \tag{1}$$

As the ansatz functions are expressed in dependency on the element coordinates s and t, the coordinates of the integral have to be transformed from x, y to s, t by means of the Jacobian matrix $\mathbf{J}$. It results equation (2) for the injected power into subsystem j averaged with respect to time which is marked by an overline. Hereby, the integral can be solved analytically in advance and then evaluated elementwise. The * states the conjugated complex value and n_L the number of loads.

$$\overline{P}_j = \sum_{e}^{n_L} \overline{P}_e = \sum_{e}^{n_L} \frac{1}{2} \int_{-1}^{1} \int_{-1}^{1} \Re\left(p_e v_e^*\right) \det \mathbf{J} \, ds \, dt \tag{2}$$

The temporal average of the kinetic and potential energy is initially calculated on the basis of elements and added together via each subsystem with respect to the load case. By means of the total energy in the m subsystems as well as the applied power injected into the individual subsystems, the matrix $\mathbf{A}$ of the energy influence coefficients can be determined (see Eq. (3)). In the following, the used parameters are averaged over time and space, which is not explicitly marked by an overline for readability.

$$\mathbf{A} = \mathbf{E}\mathbf{P}^{-1} = \begin{bmatrix} \frac{E_{11}}{P_1} & \frac{E_{12}}{P_2} & \cdots & \frac{E_{1m}}{P_m} \\ \frac{E_{21}}{P_1} & \frac{E_{22}}{P_2} & \cdots & \frac{E_{2m}}{P_m} \\ \vdots & \vdots & \ddots & \vdots \\ \frac{E_{m1}}{P_1} & \frac{E_{m2}}{P_2} & \cdots & \frac{E_{mm}}{P_m} \end{bmatrix} \tag{3}$$

Here, the matrix entry $A_{ij} = \frac{E_{ij}}{P_j}$ represents the energy in the subsystem i normalized to the applied power due to loading of subsystem j. It describes the energy flow inside the system and can be calculated for different load cases by Eq. (3).

Applying the Power Injection Method, another way to express the relation of the diagonal input power matrix $\mathbf{P}$ with the energy content of the subsystems $\mathbf{E}$ in the steady state is:

$$\mathbf{P} = \Omega \mathbf{L} \mathbf{E} \tag{4}$$

In Eq. (4) $\mathbf{L}$ defines the matrix of coupling and damping loss factors known from SEA. Comparing Eq. (3) with Eq. (4), the loss factor matrix $\mathbf{L}$ can be calculated by the inversion of $\mathbf{A}$. Therefore the prerequisites for an application of the SEA have to be fulfilled.

3. Robust estimation of the energy influence coefficients

In the following, the statistical behavior of the energy flow due to variation of the load will be investigated. The evaluations are performed at an L-shaped structure out of cross laminated timber - consisting of a wall and a ceiling (subsystem 1 and 2), which are modeled by volume elements [5].

3.1 Rain-on-the-Roof

The EFA offers the possibility to compute either the energy influence coefficients for a specific load scenario or - in case the load is unknown - for a so-called Rain-on-the-Roof (RotR) excitation. The latter shall lead to robust energy influence coefficients which are as representative as possible for an unknown load. Therefore, RotR shall ensure the participation of all modes in the system response. Furthermore, the excitation shall be statistically independent to avoid a coherent modal response and to fulfill the SEA assumption of equipartition of modal energy. Therefore, RotR consists of several single loads with unity magnitude and a random phase. [4]

The direct field of vibration due to a point excitation is dominating over the reverberant field within the reverberation radius. From a modal point of view the direct field is described by resonant and non-resonant modes. In contrast to the SEA the EFA directly copes with non-resonant transmission. If a sufficiently large number of nodes within a subsystem is excited with a random phase, the subsystem energy can be represented by the reverberant energy by taking two times the kinetic energy according to the SEA assumption. On the one hand, to do a comparison with the SEA it is convenient to fulfill its assumptions. On the other hand, the consideration of the non-resonant transmission states a benefit of the EFA as it models vibroacoustic problems more realistically. E.g., by modeling plates with several layers of volume elements the location of the load across the thickness can be taken into account and consequently thickness modes might be excited. Furthermore, its effect on the energy flow containing non-resonant transmission can be shown [5].

To perform a RotR excitation, different approaches have been presented in literature. Mace [6] proposes a load vector whose amplitude is proportional to the local mass density of the corresponding subsystem. Hence, all subsystem modes are excited by equal modal forces, such, that the direct wavefield receives a uniform power input. To make the excitation incoherent, it is spatially delta-correlated. This modal approach is part of a component-mode synthesis [2], which is convenient for problems with a limited number of subsystem modes.

3.2 Averaging per frequency band and over realizations

Above the first antisymmetric mode of thickness-shear the number of modes is increasing significantly. Especially for wooden plates this limit already occurs at comparatively low frequencies as its Young's modulus perpendicular to the fiber is about one thirtieth of the one in fiber direction. In this case it is computationally more efficient to perform a harmonic analysis where the complex

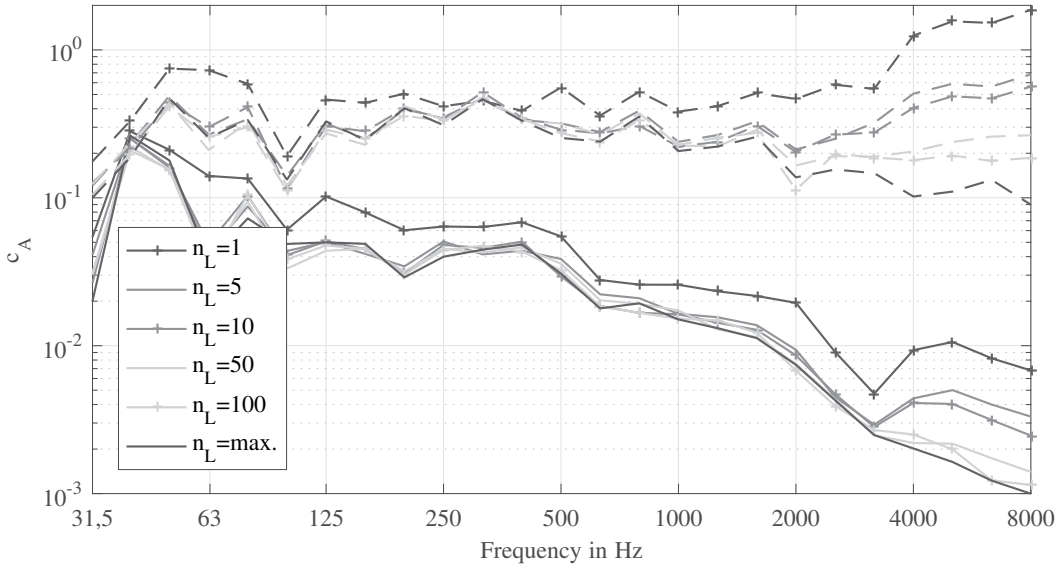

Figure 1: Coefficients of variation of A_{12} (- -) and A_{22} (—) based on 100 realizations for different numbers of loads n_L; n_L=max. corresponds to loading each element per subsystem.

dynamic stiffness matrix is inverted and solved for certain frequencies of excitation f. To cover the whole frequency range of interest - e.g. the extended one for building acoustics from 50 to 5000 Hz - a logarithmically equidistant spacing between the excited frequencies is proposed. This leads to an identical number of evaluated frequencies n_f for each one-third octave band.

To obtain the band averaged energy influence coefficients the time averaged subsystem energies and the corresponding input power are summed up within each band and inserted into Eq. (3). Equation (**??**) shows the resulting matrix entries where the average per frequency band is marked by a second overline. Inverting the resulting matrix leads to the band averaged coupling loss factors according to section 2. If a structure is characterized by energy influence coefficients the energy flow into the different subsystems can be predicted for a certain input power. Hence, this relation is only true for band averaged values if the subsystem energies and the input power were summed separately before computing the energy influence coefficients. This corresponds to the weighted arithmetic mean of the energy influence coefficient with respect to the input power:

$$\overline{\overline{A_{ij}}} = \frac{\overline{\overline{E_{ij}}}}{\overline{\overline{P_j}}} = \frac{\sum_f^{n_f} E_{ij}^f}{\sum_f^{n_f} P_j^f} = \frac{\sum_f^{n_f} A_{ij}^f P_j^f}{\sum_f^{n_f} P_j^f} = \frac{A_{ij}^1 P_j^1 + A_{ij}^2 P_j^2 + \ldots + A_{ij}^{n_f} P_j^{n_f}}{P_j^1 + P_j^2 + \ldots + P_j^{n_f}} \tag{5}$$

As mentioned in section 2, in the present examinations, instead of using nodal loads, pressure is applied on selected elements to avoid singularities. Loading each element (n_L=max.) perpendicular to the surface with the same pressure and a random phase results in an approximation of a spatially delta-correlated excitation. Hence, due to loading at the surface and unlike SEA a non-resonant excitation of thickness modes is induced [5]. To quantify the influence of the random phase on the energy influence coefficient its statistical behavior is investigated by comparing different realizations of the above mentioned loading. Figure **??** shows the coefficient of variation c_A which is a relative measure as it normalizes the sample standard deviation s_A by the sample mean $\overline{A}$ (cf. Eq. (5) to (7)). Therefore, the notation of the band averaged energy influence coefficient of one realization r (cf. Eq. (**??**)) is first complemented and then purified: $\overline{\overline{A_{ij}}} = \overline{\overline{A_{ij}^r}} = A^r$.

$$\widehat{\mathrm{E}}\left[A\right] = \overline{A} = \frac{1}{n}\sum_{r=1}^{n} A^r \tag{6}$$

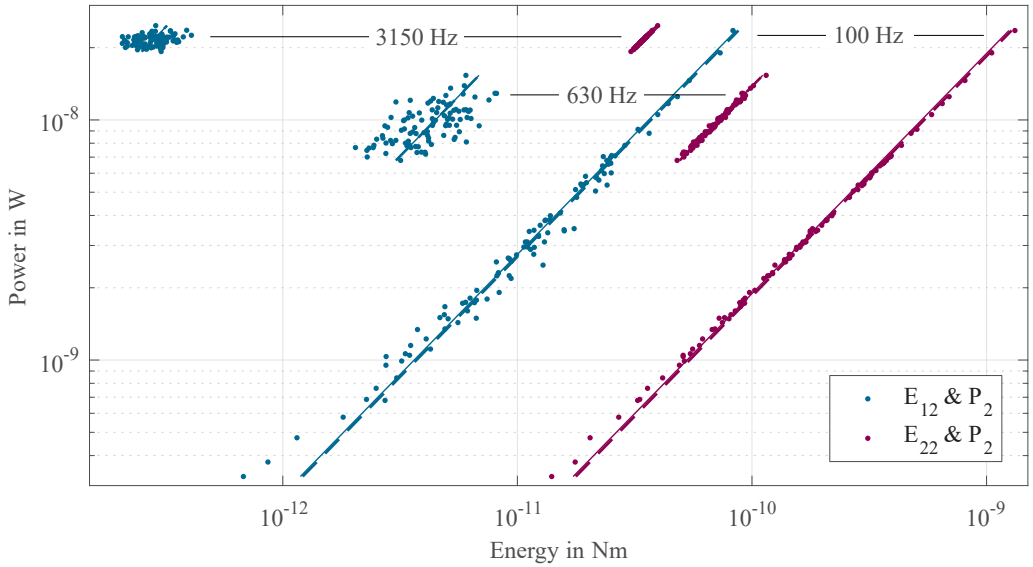

Figure 2: Power vs. energy (n=100, n_L=max.): $\overline{A}$ (—), $\overline{A}$ weighted by power (- -); from right to left: 100 Hz ($\rho_{12} = 0.99, \rho_{22} = 1.0$), 630 Hz ($\rho_{12} = 0.61, \rho_{22} = 1.0$) and 3150 Hz ($\rho_{12} = 0.25, \rho_{22} = 1.0$).

$$\widehat{\mathrm{Var}}\left[A\right] = s_A^2 = \frac{1}{n-1}\sum_{r=1}^{n}\left(A^r - \overline{A}\right)^2 \tag{7}$$

$$c_A = \frac{s_A}{\overline{A}} \tag{8}$$

Hence, unlike the weighted averaging per frequency band, the average over n different realizations is performed unweighted. The latter technique is chosen due to reasons of simplicity regarding further statistical evaluations. If the power is used as a weighting factor, this will lead to an additional correlated random variable in Eq. (**??**). Equation (8) shows the relationship between the two averaging techniques by an second order Taylor series expansion, where ρ_{EP} denotes the Pearson correlation coefficient between energy and power. The expression in the inner brackets scaled by c_P, the coefficient of variation of the power, makes the difference. As c_P becomes small with increasing frequency the two averaging techniques differ only slightly at low frequencies comparing the standard deviation and the mean (cf. Fig. 1).

$$\overline{A} = \widehat{\mathrm{E}}\left[A\right] = \widehat{\mathrm{E}}\left[\frac{E}{P}\right] \approx \frac{\overline{E}}{\overline{P}}\left(1 + c_P\left(c_P - \rho_{EP}\, s_E\right)\right) \tag{9}$$

3.3 Confidence interval of the true mean - number of realizations

The upcoming question is, if the true mean of the energy influence coefficient μ_A can be estimated with a certain precision by averaging over an affordable number of realizations n_{min}. One possible measure is the confidence interval which potentially includes the true mean. If the execution of n_{min} realizations is repeated, the confidence level describes for how many cases the interval will include the true mean. A certain confidence level of $(1-\alpha)$ is related to a confidence interval I by $\Pr(\mu_A \in I) = 1 - \alpha$. Hence, the $100\,(1-\alpha)$ % confidence interval for the true mean results in [7]:

$$\overline{A} - t_{(1-\frac{\alpha}{2})}\frac{s_A}{\sqrt{n}} < \mu_A < \overline{A} + t_{(1-\frac{\alpha}{2})}\frac{s_A}{\sqrt{n}} \tag{10}$$

whereat the variance of the sample mean $\overline{A}$ is estimated by:

$$\widehat{\mathrm{Var}}[\overline{A}] = \frac{\widehat{\mathrm{Var}}\left[A\right]}{n} = \frac{s_A^2}{n} \tag{11}$$

In Eq. (9) $z_{(1-\frac{\alpha}{2})}$ describes the $(1-\frac{\alpha}{2})$ quantile of Student's t-distribution with $n-1$ degrees of freedom. Equation 9 is based on the assumption that the mean value follows a normal distribution with $\overline{A} \sim \mathcal{N}(\mu_A, \frac{\sigma_A}{\sqrt{n}})$. This holds accordingly to the central limit theorem as the energy influence coefficient can be considered as independent and identically distributed random variable. As the sample standard deviation is used to replace the true one, the quantile values are taken from the t-distribution instead of the normal distribution. Inserting Eq. (7) in Eq. (9) leads to the following limits of the confidence interval:

$$\overline{A}\left(1 \mp t_{(1-\frac{\alpha}{2})}\frac{c_A}{\sqrt{n}}\right) \tag{12}$$

There are different possibilities to characterize the uncertainty. As the energy influence coefficient shows a high variation in magnitude over the entire frequency range, a relative, logarithmic deviation is chosen as a measure. Hence, the level difference between the sample and the true mean should be smaller than the relative error D:

$$|L_{\overline{A}} - L_{\mu_A}| < D \qquad \text{with } L_A = 10\lg\left(\frac{A}{A_{\text{ref}}}\right) \text{ and } A_{\text{ref}} = 10^{-12}. \tag{13}$$

Expression (11) can be rewritten as:

$$\left|10\lg\frac{\overline{A}}{\mu_A}\right| < D \qquad \Leftrightarrow \quad -D < 10\lg\frac{\overline{A}}{\mu_A} < D$$

After some transformations the following interval results:

$$\Leftrightarrow \quad \underbrace{\left(1-10^{\frac{D}{10}}\right)\frac{\sqrt{n}}{c_A}}_{t_l} < \underbrace{\frac{\overline{A}-\mu_A}{\frac{s_A}{\sqrt{n}}}}_{:=T\sim t_{n-1}} < \underbrace{\left(1-10^{\frac{-D}{10}}\right)\frac{\sqrt{n}}{c_A}}_{t_u}$$

If expression (11) should be fulfilled with a probability of $(1-\alpha)$, it holds equivalently:

$$\begin{aligned} &\Pr\left(|L_{\overline{A}} - L_{\mu_A}| < D\right) = 1-\alpha \\ \Leftrightarrow\ &\Pr\left(t_l < T < t_u\right) = 1-\alpha \\ \Leftrightarrow\ &F_T\left(t_u\right) - F_T\left(t_l\right) = 1-\alpha \end{aligned} \tag{14}$$

Expression (12) either delivers n_{min} by solving it numerically or is evaluated for explicit values of n, D and c_A to be depicted in contour plots like in Fig. 2. These curves are calculated based on the maximum coefficient of variation in Fig. **??**, $c_A = 0.5$, considering the entire frequency range and an excitation with greater or equal 5 loads. Choosing e.g. a maximum deviation of $D = 1$ dB from the true mean a simulation consisting of a minimum number of $n = 37$ realizations has to be performed that - repeating the simulation several times - in 99 % of the repetitions the true mean lies within the corresponding confidence interval. In case the required number of realizations becomes small the prerequisites of the presented procedure might be violated.

3.4 Number of loads - coefficient of variation

Loading each element (n_L=max.) at each frequency step leads to a high computational effort which is attempted to be minimized. Therefore, the number of loads shall be reduced. To be able to quantify its influence on each of five different numbers of loads 100 realizations are performed. The criteria for the RotR excitation are still fulfilled as the forces are statistically independent to produce an incoherent modal response and subsequently equipartition of modal energy.

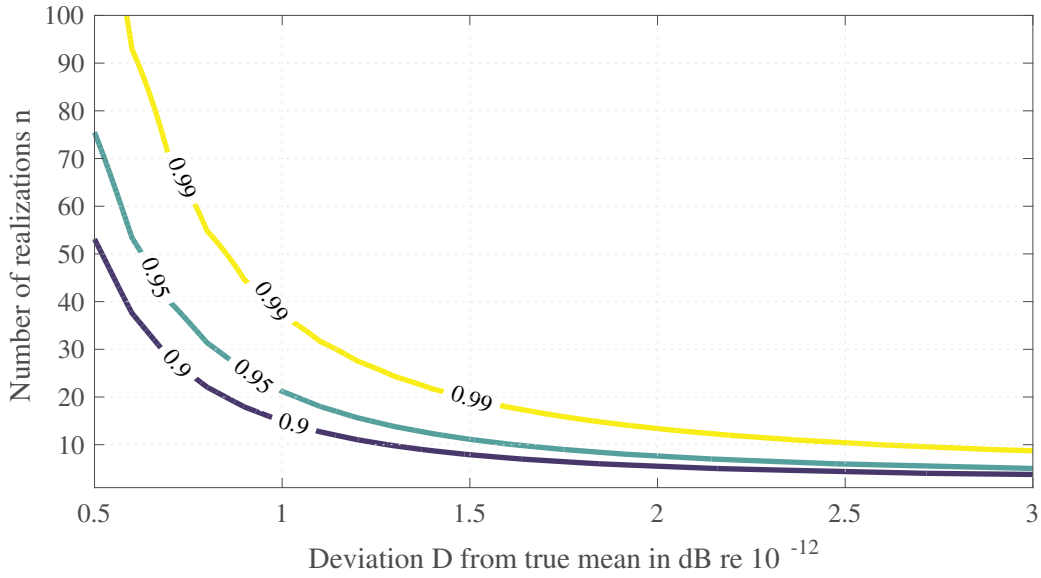

Figure 3: Number of realizations n for the deviation D from the true mean μ_A based on $c_A = 0.5$.

Figure **??** shows the coefficient of variation for different numbers of loads. An increasing number of loads leads to a lower coefficient of variation for the energy influence coefficients A_{12} and A_{22}. The single load leads to a significantly higher deviation between the individual realizations over the entire frequency range. For several loads per realization the first thickness-shear resonances of the excited plate 2 at 1370 and 1823 Hz state the lower limit of different levels according to the number of loads [5]. Hence, at the first thickness-stretch resonance of 3860 Hz the curves are already well separated. At low frequencies one-third octave bands with few or none resonant modes might also lead to deviations. The coefficient of variation of the power P_2 decreases with increasing frequency as the locations of the loads become less decisive for shorter wavelengths. As P_2 is fully correlated over the entire frequency range with the energy in the excited subsystem E_{22} its coefficient of variation and the one of A_{22} behave analogously. Due to a decreasing correlation coefficient ρ_{12} of P_2 and E_{12} the variation of A_{12} behaves different. It remains in the same magnitude below the thickness resonances.

Figure 1 presents the relationship between the input power and the energy in the excited and the adjacent subsystem, respectively, for 100 realizations with a varying excitation pattern (n_L=max.). Three selected one-third octave bands are depicted. The global modes in the 100 Hz one-third octave band lead to a high correlation of the input power with the energy in the excited and the indirectly excited subsystem, too. This definite relationship holds for the higher one-third octave bands only in the excited subsystem. It seems that in the non-excited one the energy behaves nearly independent of the injected power as the individual realizations form a cloud instead of a line. This indicates that the subsystems are weakly coupled. Compared to the excited subsystem the energetic level is orders of magnitudes smaller. It is assumed that the latter is influenced by the varying excitation pattern.

3.5 Sample mean - comparison to SEA

Whereas the arithmetic sample mean of the energy influence coefficients A_{22} and A_{12} shows at low frequencies some small deviations for different numbers of loads, the thickness modes lead for the latter one to slightly different levels at high frequencies (cf. Fig 3).

In addition, the structure is investigated by SEA whereat the rigid connection of wall and ceiling is modeled by a line coupling. Exciting the bending waves in subsystem 2 leads to an almost identical ensemble average for the normalized energy in the excited subsystem (A_{22}). The normalized energy in the adjacent subsystem A_{12} is overestimated at low and high frequencies as the assumptions of the SEA and of the Mindlin wave approximation are not fulfilled, respectively [8].

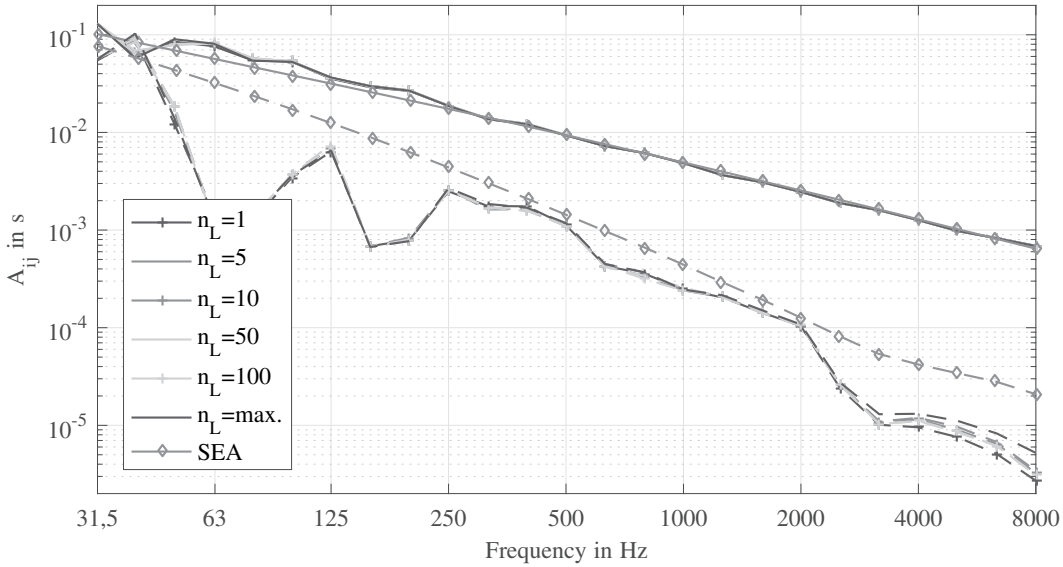

Figure 4: Sample mean value of A_{12} (- -) and A_{22} (—) based on 100 realizations of different numbers of loads n_L compared to the ensemble average from SEA.

4. Conclusion

In case the load is unknown a robust estimation of the energy flow is needed for a general prediction of sound transmission. The SEA delivers an ensemble average within a limited frequency range. The EFA can also be applied at low frequencies with a small amount of modes as well as at high frequencies taking thickness modes into account. One realization of the EFA delivers a prediction for one specific load case. By averaging over varying random load cases a robust energy flow with respect to the load can be predicted. A procedure is shown to find a minimum number of realizations to compute energy influence coefficients within a certain confidence interval. Furthermore, it can be applied to other random variables like coupling loss factors by considering their statistical behavior. In addition, other uncertainties can be covered like choosing the material data as random input variables.

REFERENCES

1. Lyon, R. H. and DeJong, R. G., *Theory and application of statistical energy analysis*, Butterworth-Heinemann, Boston et al, 2. edn. (1995).

2. Mace, B. R. and Shorter, P. J. Energy flow models from finite element analysis, *Journal of Sound and Vibration*, **233** (3), 369–389, (2000).

3. Winter, C. et al. Modelling the sound transmission across junctions of building components by energy influence coefficients, *IX International Conference on Structural Dynamics*, (2014).

4. Hopkins, C., *Sound insulation: Theory into Practice*, Butterworth-Heinemann, Oxford, 1st ed. edn. (2007).

5. Winter, C. et al. Modeling of orthotropic plates out of cross laminated timber in the mid and high frequency range, *X International Conference on Structural Dynamics*, (2017).

6. Mace, B. Statistical energy analysis, energy distribution models and system modes, *Journal of Sound and Vibration*, **264** (2), 391–409, (2003).

7. Papaioannou, I., *Stochastic Finite Element Methods*, Technical University of Munich (2016).

8. Winter, C. et al. Beschreibung des Energieflusses über Stoßstellen leichter Massivholzkonstruktionen im mittleren und höheren Frequenzbereich, *43. Jahrestagung für Akustik*, (2017).